Interfacial Binding Dynamics of Bee Venom Phospholipase A(2) Investigated by Dynamic Light Scattering and Quartz Crystal Microbalance

ARTICLE *in* LANGMUIR · DECEMBER 2009

Impact Factor: 4.46 · DOI: 10.1021/la903117x · Source: PubMed

4 AUTHORS, INCLUDING:

Curtis W. Frank
Stanford University
363 PUBLICATIONS **10,070** CITATIONS

Langmuir
Article
pubs.acs.org/Langmuir

Interfacial Binding Dynamics of Bee Venom Phospholipase A_2 Investigated by Dynamic Light Scattering and Quartz Crystal Microbalance

Joshua A. Jackman,[§] Nam-Joon Cho,[†,‡] Randolph S. Duran,[§] and Curtis W. Frank*[,†]

[†]*Department of Chemical Engineering, and* [‡]*Department of Medicine, Division of Gastroenterology and Hepatology, School of Medicine, Stanford University, Stanford, California, 94305, and* [§]*Department of Chemistry, University of Florida, Gainesville, Florida, 32611*

Received August 21, 2009. Revised Manuscript Received November 16, 2009

Bee venom phospholipase A_2 ($bvPLA_2$) is part of the secretory phospholipase A_2 ($sPLA_2$) family whose members are active in biological processes such as signal transduction and lipid metabolism. While controlling $sPLA_2$ activity is of pharmaceutical interest, the relationship between their mechanistic actions and physiological functions is not well understood. Therefore, we investigated the interfacial binding process of $bvPLA_2$ to characterize its biophysical properties and gain insight into how membrane binding affects interfacial activation. Attention was focused on the role of membrane electrostatics in the binding process. Although dynamic light scattering experiments indicated that $bvPLA_2$ does not lyse lipid vesicles, a novel, nonhydrolytic activity was discovered. We employed a supported lipid bilayer platform on the quartz crystal microbalance with dissipation sensor to characterize this bilayer-disrupting behavior and determined that membrane electrostatics influence this activity. The data suggest that (1) adsorption of $bvPLA_2$ to model membranes is not primarily driven by electrostatic interactions; (2) lipid desorption can follow $bvPLA_2$ adsorption, resulting in nonhydrolytic bilayer-disruption; and (3) this desorption is driven by electrostatic interactions. Taken together, these findings provide evidence that interfacial binding of $bvPLA_2$ is a dynamic process, shedding light on how membrane electrostatics can modulate interfacial activation.

Introduction

Biological membranes play active roles in the regulation of many important cellular processes and also serve as protective barriers.[1−4] Many organic and inorganic species interact with membranes, which are primarily composed of a phospholipid bilayer along with numerous other components including cholesterol, membrane proteins, steroids, and glycolipids.[1,2,5] Cell membranes are generally negatively charged,[4,6,7] and both the charge distribution and charge density of the membrane can play important roles in membrane-protein interactions.[8,9] We sought to understand how the electrical properties of membranes affect the binding interaction of bee (*Apis mellifera*) venom phospholipase A_2 ($bvPLA_2$), which is a member of the 13−18 kDa secreted phospholipase A_2 (PLA_2) family.[10−13]

The even larger PLA_2 superfamily consists of a diverse set of enzymes that catalyze the hydrolysis of the *sn*-2 ester bond of phospholipids to produce free fatty acids and lysophospholipids.[11] Different members of the PLA_2 family play important roles in biological processes such as signal transduction[14] and eicosanoid production for inflammatory response,[15] as well as act as bactericides.[16] Secretory PLA_2 ($sPLA_2$) is one of two major classes of PLA_2, and its members have a catalytic mechanism that requires a Ca^{2+} ion in the active site.[11,17]

Although a Ca^{2+} ion is a required cofactor for an $sPLA_2$ to bind a lipid molecule to the active site and for the subsequent chemical reaction step, it is not necessary for the initial step in which the enzyme binds to a phospholipid interface from bulk solution.[10] Interfacial binding is mediated by the interaction between the enzyme's interface binding surface (defined as the i-face),[13] which surrounds the hydrophobic pocket leading to the active site, and the phospholipid interface. In contrast to the active site structure that is highly conserved across all $sPLA_2$ members,[11] the i-face structure is more varied.[10] This has led to speculation that the specific yet diverse functions of $sPLA_2$s are caused by attractive interactions with different phospholipid interfaces depending on the structural properties of the i-face.[10,18−20] Although interfacial binding is necessary for the subsequent kinetic steps and its selectivity provides insight into the wide range of $sPLA_2$ functions, the biophysical mechanism behind this process is not well understood.[20−24]

*To whom correspondence should be addressed. Professor Curtis W. Frank Department of Chemical Engineering, Stanford University, 381 North-South Mall, Stauffer III, Stanford, California, 94305. E-mail: curt.frank@stanford.edu.

(1) Conner, S. D.; Schmid, S. L. *Nature* **2003**, *422*, (6927), 37−44.
(2) Simons, K.; Toomre, D. *Nat. Rev. Mol. Cell Biol.* **2000**, *1*, (1), 31−39.
(3) Singer, S. J.; Nicolson, G. L. *Science* **1972**, *175*, (23), 720−731.
(4) Steyer, J. A.; Almers, W. *Nat. Rev. Mol. Cell Biol.* **2001**, *2*, (4), 268−275.
(5) Tanford, C. *Science* **1978**, *200*, (4345), 1012−1018.
(6) Cevc, G. *Biochim. Biophys. Acta* **1990**, *1031*, (3), 311−382.
(7) McLaughlin, S. *Annu. Rev. Biophys. Biophys. Chem.* **1989**, *18*, 113−36.
(8) McLaughlin, S.; Murray, D. *Nature* **2005**, *438*, (7068), 605−611.
(9) Sakai, N.; Matile, S. *Chemistry* **2000**, *6*, (10), 1731−1737.
(10) Berg, O. G.; Gelb, M. H.; Tsai, M. D.; Jain, M. K. *Chem Rev* **2001**, *101*, (9), 2613−2654.
(11) Dennis, E. A. *J. Biol. Chem.* **1994**, *269*, (18), 13057−13060.
(12) Gelb, M. H.; Jain, M. K.; Hanel, A. M.; Berg, O. G. *Annu. Rev. Biochem.* **1995**, *64*, 653−688.
(13) Ramirez, F.; Jain, M. K. *Proteins: Struct., Funct., Genet.* **1991**, *9*, (4), 229−239.
(14) Dennis, E. A.; Rhee, S. G.; Billah, M. M.; Hannun, Y. A. *FASEB J* **1991**, *5*, (7), 2068−2077.
(15) Balsinde, J.; Balboa, M. A.; Insel, P. A.; Dennis, E. A. *Ann. Rev. Pharmacol. Toxicol.* **1999**, *39*, 175−189.
(16) Qu, X. D.; Lehrer, R. I. *Infect. Immun.* **1998**, *66*, (6), 2791−2797.
(17) Burke, J. E.; Dennis, E. A. *J. Lipid Res.* **2009**, *50* Suppl, S237−S242.
(18) Scott, D. L.; White, S. P.; Otwinowski, Z.; Yuan, W.; Gelb, M. H.; Sigler, P. B. *Science* **1990**, *250*, (4987), 1541−1546.
(19) Scott, D. L.; Sigler, P. B. *Adv. Protein Chem.* **1994**, *45*, 53−88.
(20) Winget, J. M.; Pan, Y. H.; Bahnson, B. J. *Biochim. Biophys. Acta* **2006**, *1761*, (11), 1260−1269.
(21) Tatulian, S. A. *Biophys. J.* **2001**, *80*, (2), 789−800.
(22) Tatulian, S. A.; Biltonen, R. L.; Tamm, L. K. *J. Mol. Biol.* **1997**, *268*, (5), 809−815.
(23) Han, S. K.; Yoon, E. T.; Scott, D. L.; Sigler, P. B.; Cho, W. *J. Biol. Chem.* **1997**, *272*, (6), 3573−3582.
(24) Gelb, M. H.; Cho, W.; Wilton, D. C. *Curr. Opin. Struct. Biol.* **1999**, *9*, (4), 428−432.

There is currently debate over what types of interactions, including electrostatic, hydrogen bonding, and hydrophobic interactions, modulate interfacial binding.[10,24−27] Changing membrane structural parameters such as surface charge can affect the binding affinity of $sPLA_2$s,[21,23,25] which consequently affects the interfacial activation process. Tatulian et al.[22] suggest that "interfacial activation should be interpreted in a somewhat different way, dividing it into the 'interfacial binding' and 'activation' steps". This article focuses on the biophysical interaction between $bvPLA_2$ and model membranes of varying surface charge to examine how membrane electrostatics affect interfacial binding, including the type of binding interaction, and subsequent interfacial activation.

In addition to monitoring vesicle size changes associated with enzymatic activity (i.e., lipolysis and self-assembly of the lipolytic products) under catalytic conditions (i.e., in the presence of the Ca^{2+} cofactor), dynamic light scattering (DLS) experiments were used to determine how the membrane interaction of $bvPLA_2$ under initially noncatalytic conditions (i.e., in the absence of the Ca^{2+} cofactor required for enzymatic activity) affected its enzymatic activity following Ca^{2+} addition.

To further investigate the binding interaction of $bvPLA_2$ under noncatalytic conditions, we employed a solid-supported lipid bilayer platform on the quartz crystal microbalance with dissipation (QCM-D) sensor to monitor the binding dynamics.[28−30] This bilayer platform has been previously used as a model cell membrane for other $sPLA_2$ studies.[21,31−35] QCM-D is a popular tool for probing the mass and viscoelastic properties of thin films with nanogram sensitivity.[36−38] Recent studies have shown that QCM-D is a highly effective tool for studying biomacromolecular interactions in the liquid state, notably in systems with highly specific adsorption.[28,39−41]

In this article, we reveal a dynamic, two-step process to describe the binding interaction of $bvPLA_2$ with negatively charged phospholipid interfaces. To the best of our knowledge, this mechanism provides novel insight into how membrane electrostatics can modulate enzymatic activity. While membrane adsorption of $bvPLA_2$ is not driven primarily by electrostatics, subsequent lipid desorption, which is linked to the bilayer-disrupting activity of $bvPLA_2$, is significantly affected by membrane electrostatics. Specifically, a novel, nonhydrolytic bilayer-disrupting activity of $bvPLA_2$ targets anionic membranes, triggering a change in bilayer topology that has previously been considered primarily in the context of lateral phase separation resulting from small-scale lipolysis.[42,43] Therefore, this finding links together two known determinants of interfacial activation, bilayer topology and anionic lipid fraction, to explain the well-established experimental finding of increased $sPLA_2$ activity toward anionic membranes.[13,44] By employing a model membrane platform together with the surface-sensitive QCM-D technique, we have demonstrated that membrane adsorption is a necessary but insufficient step for subsequent enzymatic activity. A novel electrostatically driven interaction between $bvPLA_2$ and lipid membranes was discovered that is sufficient for interfacial activation. While this study focuses on $bvPLA_2$, we expect a similar mechanism of interfacial activation to be conserved across evolutionarily similar $sPLA_2$s.

Materials and Methods

Bee Venom Phospholipase A_2 ($bvPLA_2$). A lyophilized, dry powder form of $sPLA_2$ derived from bee (*Apis mellifera*) venom (Sigma-Aldrich, St. Louis, MO, U.S.A.) was stored at −20 °C. The enzyme, which has a pI value of 7.8,[45] was hydrated in Tris buffer (10 mM Tris [pH 7.7], 150 mM NaCl, and 2 mM EDTA) at a stock concentration of 1 $mg \cdot mL^{-1}$ and was stored at 4 °C before the experiment. Following hydration, $bvPLA_2$ was used for experiments within twenty-four hours.

Small Unilamellar Vesicle Preparation. Small unilamellar vesicles of varying molar ratios of 1,2-dioleoyl-*sn*-glycero-3-phosphatidylserine (DOPS), 1,2-dioleoyl-*sn*-glycero-3-phosphatidylcholine (DOPC), and 1,2-dioleoyl-*sn*-glycero-3-ethylphosphocholine (DOEPC) (Avanti Polar Lipids, Alabaster, AL, U.S.A.) were prepared by the extrusion method, as previously described.[46]

Vesicle solutions for ζ-potential measurements were diluted in Tris buffer (10 mM Tris [pH 8.0] and 150 mM NaCl). Vesicle solutions for DLS experiments were diluted in Tris buffer (10 mM Tris [pH 8.0], 150 mM NaCl, and 2 mM EDTA). For QCM-D experiments, vesicle solutions were diluted with Tris buffer (10 mM Tris [pH 7.7], 150 mM NaCl, and 2 mM EDTA). An identical Tris buffer but with 250 mM NaCl was initially used for QCM-D experiments involving DOPS-containing vesicles in order to create a high osmotic pressure across the bilayer to promote substrate-mediated vesicle rupture. All aqueous solutions and buffers were prepared in Milli-Q water with a minimum resistivity of 18.2 MΩ·cm (Millipore, Billerica, MA, U.S.A.).

ζ-Potential. The electrophoretic mobility of vesicles in solution was measured to calculate the vesicle ζ-potential. A ZetaPals analyzer (Brookhaven Instruments, Holtsville, NY, U.S.A) with a 658.0 nm monochromatic laser was used for all measurements. The measurements were performed in Tris buffer (10 mM Tris [pH 8.0] and 10 mM NaCl), and the temperature was set at 24.0 °C for all experiments.

Dynamic Light Scattering (DLS). DLS measurements recorded changes in vesicle size distribution as the result of interactions between $bvPLA_2$ and vesicles. All initial vesicle size measurements were performed in Tris buffer (10 mM Tris [pH 8.0], 150 mM NaCl, and 2 mM EDTA), and the temperature was set at 25.0 °C. For experiments in which the interaction between $bvPLA_2$ and vesicles under catalytic conditions was

(25) Scott, D. L.; Mandel, A. M.; Sigler, P. B.; Honig, B. *Biophys. J.* **1994**, *67*, (2), 493−504.
(26) Bollinger, J. G.; Diraviyam, K.; Ghomashchi, F.; Murray, D.; Gelb, M. H. *Biochemistry* **2004**, *43*, (42), 13293−13304.
(27) Ghomashchi, F.; Lin, Y.; Hixon, M. S.; Yu, B. Z.; Annand, R.; Jain, M. K.; Gelb, M. H. *Biochemistry* **1998**, *37*, (19), 6697−6710.
(28) Cho, N. J.; Cheong, K. H.; Lee, C.; Frank, C. W.; Glenn, J. S. *J. Virol.* **2007**, *81*, (12), 6682−6689.
(29) Keller, C. A.; Glasmastar, K.; Zhdanov, V. P.; Kasemo, B. *Phys. Rev. Lett.* **2000**, *84*, (23), 5443−5446.
(30) Keller, C. A.; Kasemo, B. *Biophys. J.* **1998**, *75*, (3), 1397−1402.
(31) Vacklin, H. P.; Tiberg, F.; Fragneto, G.; Thomas, R. K. *Biochemistry* **2005**, *44*, (8), 2811−2821.
(32) Justesen, P. H.; Kristensen, T.; Ebdrup, T.; Otzen, D. *J. Colloid Interface Sci.* **2004**, *279*, (2), 399−409.
(33) Grandbois, M.; Clausen-Schaumann, H.; Gaub, H. *Biophys. J.* **1998**, *74*, (5), 2398−2404.
(34) Nielsen, L. K.; Risbo, J.; Callisen, T. H.; Bjornholm, T. *Biochim. Biophys. Acta* **1999**, *1420*, (1−2), 266−271.
(35) Wacklin, H. P.; Tiberg, F.; Fragneto, G.; Thomas, R. K. *Biochim. Biophys. Acta* **2007**, *1768*, (5), 1036−1049.
(36) Rodahl, M.; Hook, F.; Fredriksson, C.; Keller, C. A.; Krozer, A.; Brzezinski, P.; Voinova, M.; Kasemo, B. *Faraday Discuss.* **1997**, (*107*), 229−246.
(37) Rodahl, M.; Hook, F.; Kasemo, B. *Anal. Chem.* **1996**, *68*, (13), 2219−2227.
(38) Rodahl, M.; Hook, F.; Krozer, A.; Brzezinski, P.; Kasemo, B. *Rev. Sci. Instrum.* **1995**, *66*, (7), 3924−3930.
(39) Cho, N. J.; Cho, S. J.; Cheong, K. H.; Glenn, J. S.; Frank, C. W. *J. Am. Chem. Soc.* **2007**, *129*, (33), 10050−10051.
(40) Cho, N. J.; Kanazawa, K. K.; Glenn, J. S.; Frank, C. W. *Anal. Chem.* **2007**, *79*, 7027−7035.
(41) Hook, F.; Rodahl, M.; Kasemo, B.; Brzezinski, P. *Proc. Natl. Acad. Sci. U.S.A.* **1998**, *95*, (21), 12271−12276.
(42) Burack, W. R.; Dibble, A. R.; Allietta, M. M.; Biltonen, R. L. *Biochemistry* **1997**, *36*, (34), 10551−10557.
(43) Burack, W. R.; Biltonen, R. L. *Chem. Phys. Lipids* **1994**, *73*, (1−2), 209−222.
(44) Yu, B. Z.; Ghomashchi, F.; Cajal, Y.; Annand, R. R.; Berg, O. G.; Gelb, M. H.; Jain, M. K. *Biochemistry* **1997**, *36*, (13), 3870−3881.
(45) Canaan, S.; Nielsen, R.; Ghomashchi, F.; Robinson, B. H.; Gelb, M. H. *J. Biol. Chem.* **2002**, *277*, (34), 30984−30990.
(46) Armengol, X.; Estelrich, J. *J. Microencapsul*ation **1995**, *12*, (5), 525−535.

monitored, bvPLA$_2$ in Tris buffer (10 mM Tris [pH 8.0], 150 mM NaCl, and 10 mM $CaCl_2$) was added to the vesicle solution so that the final enzyme concentration was 10 $\mu g \cdot mL^{-1}$ and the final Ca^{2+} concentration was 5 mM. For experiments in which the interaction between bvPLA$_2$ and vesicles under noncatalytic conditions was monitored, bvPLA$_2$ in Tris buffer (10 mM Tris [pH 8.0], 150 mM NaCl, and 2 mM EDTA) was added to the vesicle solution so that the final enzyme concentration was 10 $\mu g \cdot mL^{-1}$. For subsequent activation of bvPLA$_2$ under initially noncatalytic conditions, a Tris buffer (10 mM Tris [pH 8.0], 150 mM NaCl, and 10 mM $CaCl_2$) was added so that the final Ca^{2+} concentration was 5 mM, resulting in a final enzyme concentration of 5 $\mu g \cdot mL^{-1}$. A 90Plus particle size analyzer (Brookhaven Instruments) with a 658.0 nm monochromatic laser was used for all measurements, and the scattering angle was set at 90° to minimize the reflection effect. The results were analyzed by digital autocorrelator software. All autocorrelation functions were also analyzed by CONTIN and nonnegatively constrained least-squares algorithms to check for multimodal distributions. All average diameter values were calculated from at least five measurements performed on each sample. For studies related to the enzymatic activity of bvPLA$_2$, 20 min time intervals were selected. The average diameter during each time interval is the average of 10 two-minute measurement cycles that were recorded over the interval.

Previous light scattering and electron microscopy studies on the interaction between sPLA$_2$ and vesicles indicate that vesicle lysis (resulting from lipolysis) and lipolytic product self-assembly caused large size changes.[42,47] However, these processes cause multimodal size distributions and fluctuations in the scattering intensity that provide only limited information about particle size. Since lipolysis can cause vesicle lysis depending on the extent of reaction, the physical state of the sample cannot be determined after the initial measurement. However, large changes in vesicle size distribution suggest enzymatic activity as bvPLA$_2$ hydrolyzes phospholipids and the lipolytic products reassemble into larger structures.

Quartz Crystal Microbalance with Dissipation (QCM-D). Membrane binding and enzymatic activity of bvPLA$_2$ were characterized by the quartz crystal microbalance with dissipation (QCM-D). Adsorption kinetics and the properties of the adsorbed layer were monitored in situ using a Q-Sense E4 (Q-Sense AB, Gothenburg, Sweden). AT-cut crystals (Q-Sense) with 14 mm diameter and 50 nm thermally evaporated silicon oxide coats were used for all QCM-D experiments. The E4 system allows for the simultaneous measurement of resonance frequency and energy dissipation changes for four individually mounted quartz crystals, as previously described.[38]

Bilayer formation and bvPLA$_2$ membrane binding experiments were performed in Tris buffer (10 mM Tris [pH 7.7], 150 mM NaCl, and 2 mM EDTA) under noncatalytic conditions. For activation of membrane-bound bvPLA$_2$, a Tris buffer (10 mM Tris [pH 7.7], 150 mM NaCl, and 5 mM $CaCl_2$) was added to the measurement chamber. A peristaltic pump was used to flow sample into the measurement chamber, with the flow rate fixed at 50 $\mu L \cdot min^{-1}$ for all experiments. The temperature of each flow cell was set at 25.0 °C and controlled by a Peltier element with fluctuations less than 0.02 °C. Each crystal was treated with oxygen plasma using a Plasma Prep 5 plasma cleaner (GaLa Instrumente GmbH, Bad Schwalbach, Germany) at ~70 W for 4 min before the experiment.

Results

Effects of Lipid Composition on Membrane Surface Potential. To study how membrane electrostatics affect the interfacial binding process of bvPLA$_2$, it was necessary to first characterize the model membrane system. Various synthetic phospholipids,

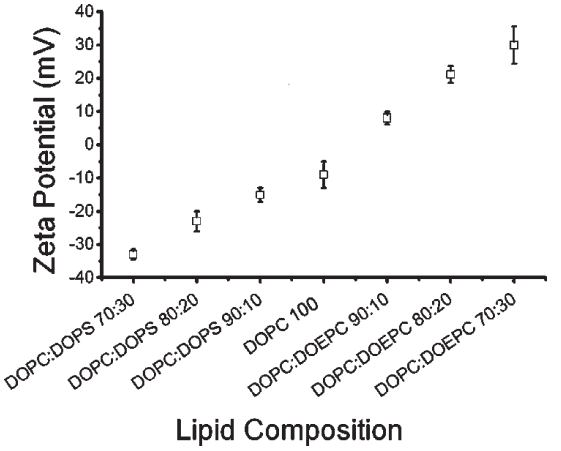

Figure 1. ζ-potential of phospholipid vesicles. Values (in mV) are recorded as a function of phospholipid composition. Each value is the average of five measurements. Error bars indicate standard deviations.

1,2-dioleoyl-*sn*-glycero-3-phosphatidylserine (DOPS), 1,2-dioleoyl-*sn*-glycero-3-phosphatidylcholine (DOPC), and 1,2-dioleoyl-*sn*-glycero-3-ethylphosphocholine (DOEPC), were mixed in different molar ratios to create lipid bilayers with well-defined electrostatic properties. Different lipid headgroups, phosphatidylcholine (PC, zwitterionic), phosphatidylserine (PS, negatively charged), and ethylphosphocholine (EPC, positively charged), were incorporated to create phospholipid bilayers with a wide range of positive and negative surface potentials. Specifically, mole fractions of DOPS or DOEPC between 0 and 30% were mixed with DOPC to form lipid vesicles.

The membrane surface potential was measured by calculating the ζ-potential from the electrophoretic mobility of vesicles in solution (average diameter ~65 nm). As shown in Figure 1, vesicle ζ-potentials ranged from -33.2 ± 1.5 mV to 30.6 ± 5.6 mV depending on the lipid composition. These values (Supporting Information Table 1, column 2) are in good agreement with those obtained from similar lipid compositions using the electrophoretic mobility technique as well.[48] Interestingly, vesicles composed of zwitterionic DOPC have a negative surface potential of -9.0 ± 4.3 mV (Figure 1), which is due to an external field created by the membrane dipole potential.[49] Fundamental characterization of the model membrane system demonstrated that the surface potential of a phospholipid bilayer could be controlled to create a well-defined platform to investigate the interfacial binding mechanism of bvPLA$_2$.

Effects of Membrane Surface Potential on the Interaction between Vesicles and bvPLA$_2$. The interaction between vesicles in bulk solution and bvPLA$_2$ was monitored by dynamic light scattering (DLS) under catalytic conditions (i.e., in the presence of free Ca^{2+}), and noncatalytic (i.e., in the absence of free Ca^{2+}) conditions. Changes in vesicle size distribution were measured in order to characterize bvPLA$_2$ binding and vesicle lysis (i.e., lipolysis). Addition of bvPLA$_2$ under catalytic conditions resulted in large changes in the vesicle size distribution of certain lipid compositions (Figure 2). Further, vesicle size distributions were not significantly affected by the addition of bvPLA$_2$ under noncatalytic conditions (Supporting Information Figure 1). However, Ca^{2+} addition to bvPLA$_2$ and vesicles under initially noncatalytic conditions resulted in size changes (Figure 3)

(47) Callisen, T. H.; Talmon, Y. *Biochemistry* **1998**, *37*, (31), 10987−10993.

(48) Kunze, A.; Svedhem, S.; Kasemo, B. *Langmuir* **2009**, *25*, (9), 5146−5158.

(49) Yang, Y.; Mayer, K. M.; Wickremasinghe, N. S.; Hafner, J. H. *Biophys. J.* **2008**, *95*, (11), 5193−5199.

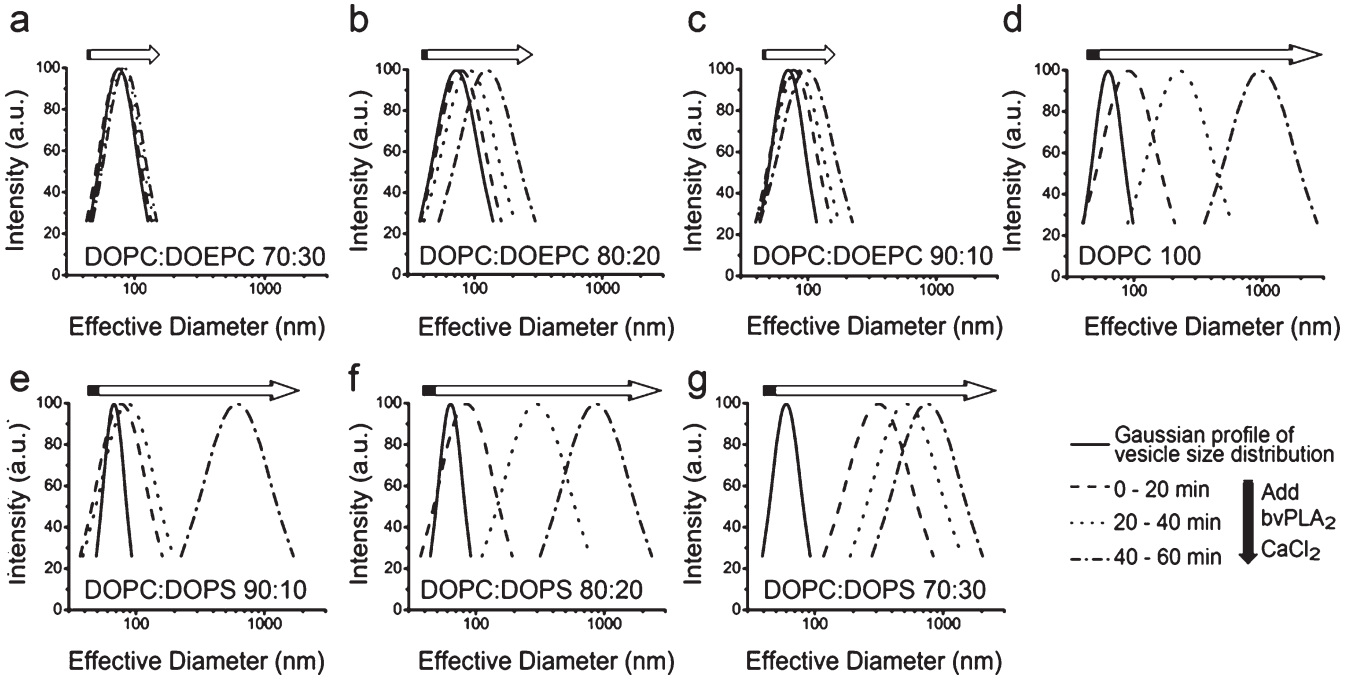

Figure 2. Effects of bvPLA$_2$ on vesicle size distribution under catalytic conditions. An initial DLS measurement of the vesicle size distribution (solid line) was recorded. Then, bvPLA$_2$ and 5 mM $CaCl_2$ were added, and size distribution measurements were recorded after 0−20 min (dashed line), after 20−40 min (dotted line), and after 40−60 min (dashed and dotted line). Corresponding size distribution changes are presented as Gaussian profiles. Arrows represent the extent of the size changes. (a) DOPC/DOEPC 70:30, (b) DOPC/DOEPC 80:20, (c) DOPC/DOEPC 90:10, (d) DOPC 100, (e) DOPC/DOPS 90:10, (f) DOPC/DOPS 80:20, and (g) DOPC/DOPS 70:30.

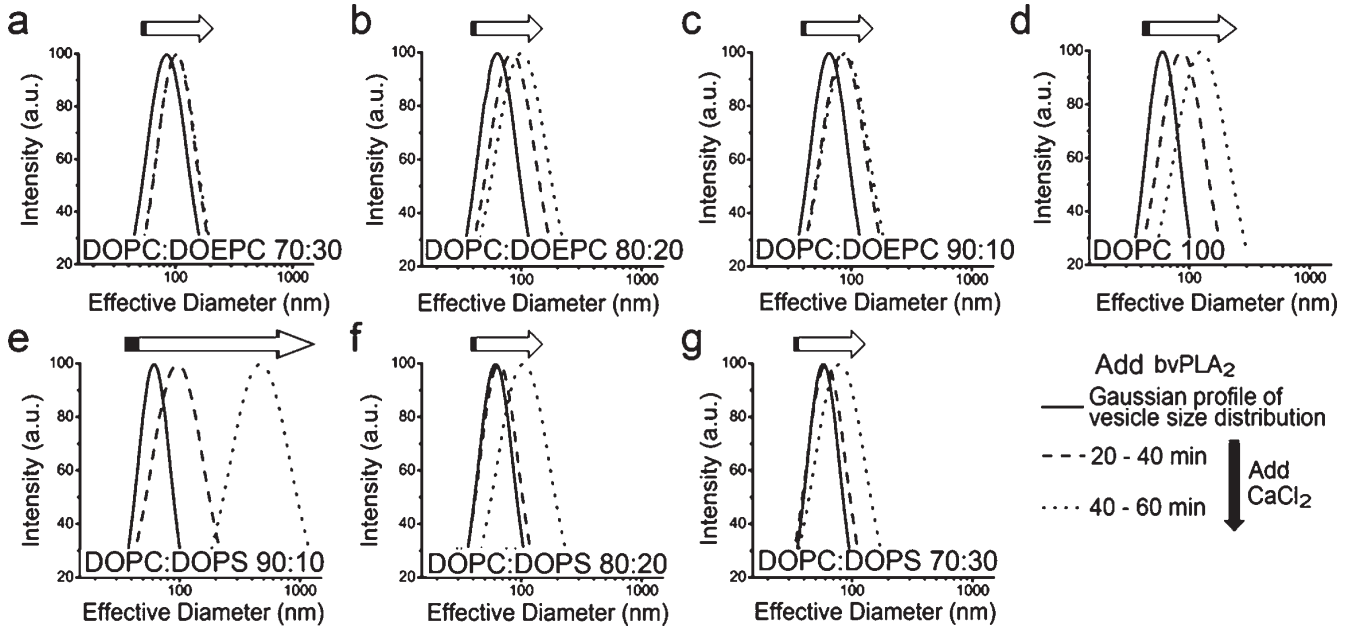

Figure 3. Ca^{2+} addition initiates enzymatic activity of bvPLA$_2$. An initial DLS measurement of the vesicle size distribution with bvPLA$_2$ under noncatalytic conditions is presented (solid line). It is replotted from the 30−40 min measurement of Supporting Information Figure 1. Then, a Tris buffer containing 5 mM $CaCl_2$ was added, and size distribution measurements were recorded 0−20 min (dashed line) and 20−40 min (dotted line) afterward. Corresponding size distribution changes are presented as Gaussian profiles. Arrows represent the extent of the size changes. (a) DOPC/DOEPC 70:30, (b) DOPC/DOEPC 80:20, (c) DOPC/DOEPC 90:10, (d) DOPC 100, (e) DOPC/DOPS 90:10, (f) DOPC/DOPS 80:20, and (g) DOPC/DOPS 70:30.

suggesting lipolytic activity. In terms of kinetics and magnitude, the size changes resulting from the addition of bvPLA$_2$ under catalytic conditions (Figure 2) and the activation of bvPLA$_2$ under initially noncatalytic conditions (Figure 3) greatly varied for certain lipid compositions. Data presented in Figures 2 and 3 indicate that the membrane interaction of bvPLA$_2$ under noncatalytic conditions affects its subsequent enzymatic activity (i.e., after Ca^{2+} addition), as described below.

Enzymatic Activity of bvPLA$_2$ under Catalytic Conditions. Vesicle size measurements were first recorded prior to addition of

bvPLA$_2$. Depending on the lipid composition, the average vesicle diameter ranged from 59.9 ± 0.4 to 75.6 ± 0.5 nm (Supporting Information Table 1, column 3). There was a general trend of increasing vesicle size with increasingly positive surface charge, although the size differences are negligible and are due to the relationship between the physical properties of each lipid composition (i.e., vesicle lysis tension) and mechanical extrusion.[50] After the initial size measurement (Figure 2a−g, solid line), bvPLA$_2$ was added under catalytic conditions and vesicle size distributions were monitored over one hour. Figure 2 presents the changes in vesicle size distribution over 0−20 min (dashed line), 20−40 min (dotted line), and 40−60 min (dashed and dotted line). From the average vesicle diameter recorded between 40 and 60 min (Supporting Information Table 1, column 4), the size change percentage was calculated (Supporting Information Table 1, column 5). Depending on the lipid composition, the size changes were either relatively small (less than 100%) or quite large (greater than 700%).

For positively charged DOPC/DOEPC vesicles, addition of bvPLA$_2$ did not significantly affect the vesicle size distribution (Figure 2a-c). During 40−60 min, the average vesicle diameter ranged from 83.8 ± 0.3 to 125.9 ± 4.0 nm (Supporting Information Table 1, column 4), corresponding to average vesicle size increases between 10.8 and 75.1% (Supporting Information Table 1, column 5). Over a longer time period, the average vesicle diameter of DOPC/DOEPC 80:20 and DOPC/DOEPC 90:10 increased to a significantly greater extent (data not shown), indicating that interfacial activation (i.e., from which time bvPLA$_2$ shows a high degree of enzymatic activity) is preceded by a long lag period (i.e., initial period of low enzymatic activity). Interestingly, the average vesicle diameter of DOPC/DOEPC 70:30 only changed 12.3% over two hours (data not shown), possibly because repulsive electrostatic interactions are too significant for membrane binding of bvPLA$_2$ to occur. The data support the conclusion that the lipolytic activity of bvPLA$_2$ can lyse positively charged vesicles, but the time before which significant size changes take place suggests a long lag period. Therefore, bvPLA$_2$ shows low enzymatic activity toward positively charged vesicles.

By contrast, bvPLA$_2$ demonstrates a high degree of enzymatic activity toward negatively charged DOPC and DOPC/DOPS vesicles. During 40−60 min, the average vesicle diameter ranged from 600.6 ± 40.5 to 856.3 ± 103.0 nm (Supporting Information Table 1, column 4), corresponding to average vesicle size increases between 791.1 and 1259.2% (Supporting Information Table 1, column 5). Surprisingly, the vesicle size distribution of zwitterionic DOPC (Figure 2d) changed faster than that of DOPC/DOPS 90:10 (Figure 2e). This increased activity toward zwitterionic membranes is possibly due to the evolution of venom sPLA$_2$s that primarily function on the outer plasma membrane, which is rich in phosphatidylcholine lipids.[51] Although this finding indicates that there are other interactions besides electrostatics that modulate enzymatic activity of bvPLA$_2$, vesicle size distributions also changed faster with increasing DOPS lipid fraction (Figure 2e−g). Past work supports this relationship since it has been shown that the lag period prior to interfacial activation can be reduced by increasing the anionic lipid fraction in a membrane.[13,44] Therefore, membrane electrostatics is an important determinant of bvPLA$_2$ activity.

Activation of bvPLA$_2$ under Initially Noncatalytic Conditions. To further characterize the interaction between vesicles and bvPLA$_2$, membrane binding was examined under noncatalytic conditions. As expected, there was little difference between vesicle size in the absence and presence of bvPLA$_2$ under noncatalytic conditions (Supporting Information Figure 1). These findings are in good agreement with a study by Canaan et al.,[45] which used a similar lipid-to-protein ratio (∼590 vs ∼375 in this study) and determined that the addition of bvPLA$_2$ to vesicles composed of the anionic lipid 1,2-ditetradecylphosphatidylmethnaol (DTPM) did not cause an increase in vesicle size or scattering intensity. Five millimolar $CaCl_2$ was then added to activate bvPLA$_2$. Initial vesicle size measurements (Figure 3, solid line) were recorded before Ca^{2+} addition. Note that the initial size measurements (Supporting Information Table 1, column 9) correspond to the measurements recorded 30−40 min after the addition of bvPLA$_2$ under noncatalytic conditions (Supporting Information Figure 1, dotted line and Supporting Information Table 1, column 8). Activation of bvPLA$_2$ initiated lipolysis, as indicated by vesicle size increases due to vesicle lysis and lipolytic product self-assembly (Figure 3). DLS measurements were recorded 0−20 min (Figure 3, dashed line) and 20−40 min (Figure 3, dotted line) after Ca^{2+} addition. Although enzymatic activity toward positively charged lipid compositions was similar in the case of bvPLA$_2$ addition under catalytic conditions (Figure 2) and after the addition of Ca^{2+} to bvPLA$_2$ under initially noncatalytic conditions, enzymatic activity toward zwitterionic and negatively charged lipid compositions was unexpectedly different depending on the addition of bvPLA$_2$ under initially catalytic or noncatalytic conditions.

Activation of bvPLA$_2$ under initially noncatalytic conditions did not result in large size changes of positively charged vesicles (Figure 3a−c) with average vesicle diameters ranging from 89.3 ± 0.8 to 102.6 ± 0.1 nm (Supporting Information Table 1, column 10) recorded 20−40 min after Ca^{2+} addition. These vesicle sizes correspond to size increases between 21.6 and 58.0% (Supporting Information Table 1, column 11). Unexpectedly, activation of bvPLA$_2$ had similar effects on most of the negatively charged vesicles (Figure 3d,f,g) except DOPC/DOPS 90:10 (Figure 3e), which had an average vesicle diameter of 425.6 ± 64.1 nm (STable 1, column 10) that corresponds to a size increase of 592.0% (Supporting Information Table 1, column 11). However, all other negatively charged vesicles had average vesicle diameters ranging from 79.5 ± 3.2 to 127.2 ± 10.7 nm (Supporting Information Table 1, column 10). These values correspond to size increases between 37.5 and 111.3% (Supporting Information Table 1, column 11). In particular, the average vesicle diameter of DOPC/DOPS 70:30 only increased from 57.8 ± 0.5 to 79.5 ± 3.2 nm, a 37.5% size increase that is within the same range as the size increases of positively charged vesicles.

Over a longer time period, the average vesicle diameter of all lipid compositions except DOPC/DOEPC 70:30 increased to a significant extent (data not shown). While the lag period is consistent with other DLS experiments for positively charged vesicles (Figure 2), there is also an increase in the lag period as the DOPS lipid fraction increases, contrary to Figure 2 and past work that demonstrated an increase in anionic lipid fraction reduces lag time.[13,44,52] To explain the differences between enzymatic activity under initially catalytic and noncatalytic conditions, membrane binding under noncatalytic conditions must either cause bvPLA$_2$ to adopt a less favorable conformation for

(50) Patty, P. J.; Frisken, B. J. *Biophys. J.* **2003**, *85*, (2), 996−1004.
(51) Kim, K. P.; Han, S. K.; Hong, M.; Cho, W. *Biochem. J.* **2000**, *348* (Pt 3), 643−647.
(52) Gadd, M. E.; Biltonen, R. L. *Biochemistry* **2000**, *39*, (32), 9623−9631.

enzymatic activity or prevent a Ca^{2+} ion (after Ca^{2+} addition) from entering the active site pocket.

Since DLS measures bulk solution properties, it is not sensitive enough to study the interfacial binding process in greater detail. Therefore, a supported lipid bilayer platform on the QCM-D sensor was employed to investigate membrane binding of $bvPLA_2$ under noncatalytic conditions and its subsequent effects on enzymatic activity.

Effects of Membrane Surface Potential on Interfacial Binding of $bvPLA_2$. Prior to experiment, a supported lipid bilayer platform of varying surface potential was formed by the surface-mediated vesicle fusion process with QCM-D monitoring (Supporting Information Figure 2). Binding data obtained under noncatalytic conditions are presented in Figure 4. At 5 min, $bvPLA_2$ was added (Figure 4a−g, arrow 1) under continuous flow for 20 min, and its membrane binding resulted in changes in the frequency response (Figure 4a−g, blue line). After an initial period of $bvPLA_2$ adsorption (Figure 4a−g, arrow 2) as indicated by the frequency decrease, the binding interaction showed unexpected desorption behavior (Figure 4c−g, arrow 3) in specific cases. Although there was significant variation in the frequency response depending on the lipid composition, the corresponding energy dissipation responses (Figure 4a−g, red line) were uniform and showed only minor changes. The small changes in energy dissipation of the bilayer platform indicated that membrane binding of $bvPLA_2$ did not significantly affect the lipid bilayer's viscoelastic properties. In addition, the minor energy dissipation changes permitted the adsorption and desorption to be described by the Sauerbrey relationship,[53] which was applied to convert the frequency changes (Hz) to binding mass values ($ng \cdot cm^{-2}$) (Table 1, columns 2 and 3).

While adsorption was similar (154.9 ± 27.3 $ng \cdot cm^{-2}$) for all lipid compositions except DOPC/DOEPC 70:30 (35.4 $ng \cdot cm^{-2}$), there was wide variance in desorption (104.9 ± 99.9 $ng \cdot cm^{-2}$). Strikingly, there was a correlation between the binding mass of desorption and the lipid composition with increased desorption for more negatively charged bilayers. To further examine this finding, the differences between the binding masses of adsorption and desorption were calculated (Table 1, column 4). In some cases, membrane binding of $bvPLA_2$ disrupted the integrity of the bilayer platform, as indicated by a decrease in the mass of the bilayer platform (Table 1, column 4, DOPC/DOPS 80:20 and DOPC/DOPS 70:30). The binding density of $bvPLA_2$ at the point of maximum adsorption (Table 1, column 5) was also calculated to examine how electrostatic interactions affect saturation of membrane binding. On the basis of the adsorption and desorption behaviors as well as bilayer-disrupting activity, three distinct types of membrane binding interaction were identified depending on lipid composition and are described below.

One-Step Adsorption Kinetics. Addition of $bvPLA_2$ to DOPC/DOEPC 70:30 resulted in a frequency shift of 2 Hz, which corresponds to 1 $bvPLA_2$ molecule per ~99 lipid headgroups (Table 1, column 5). Initially, it was hypothesized that $bvPLA_2$ would not bind to this bilayer due to a significant degree of repulsive electrostatic interactions, so this finding is surprising. In addition, it is the first report of an $sPLA_2$ binding to a positively charged membrane, supporting the conclusion that the interfacial binding energy of $bvPLA_2$ is not driven primarily by electrostatics.[26,27] While the binding density is lower than reported values,[13,54] which range from 1 $sPLA_2$ molecule per 35 to 74 lipid headgroups, one experimental difference is noteworthy. The reported values were based on binding studies with zwitterionic bilayers, whereas DOPC/DOEPC 70:30 has a significantly positive surface charge. This deviation suggests that the total amount of adsorbed $bvPLA_2$ is limited by electrostatic repulsion, which is higher when the binding density decreases. Further, no desorption was observed, unlike for all other lipid compositions. This anomaly raises the possibility that, although $bvPLA_2$ binds to DOPC/DOEPC 70:30, the type of binding interaction differs from the other lipid compositions.

Two-Step Adsorption and Desorption Kinetics. For bilayers with intermediate surface charge (DOPC/DOEPC 80:20, DOPC/DOEPC 90:10, DOPC, and DOPC/DOPS 90:10), $bvPLA_2$ initially adsorbed with maximum frequency shifts between 6 and 11 Hz (Figure 4b−e). However, there was then desorption behavior, and the final frequency shifts were between 1 and 6 Hz. The amount of desorption significantly varied (17.7−123.9 $ng \cdot cm^{-2}$) depending on the lipid composition (Table 1, column 3). There was increased desorption on more negatively charged bilayer platforms. In terms of binding density, there were ~28 lipid headgroups per $bvPLA_2$ molecule for the two positively charged bilayers (DOPC/DOEPC 80:20, and DOPC/DOEPC 90:10) (Table 1, column 5). For the two negatively charged bilayers (DOPC, and DOPC/DOPS 90:10), the binding density increased to ~20 lipid headgroups per $bvPLA_2$ molecule (Table 1, column 5). These data also suggest that the total amount of adsorbed $bvPLA_2$ is limited by electrostatic repulsion, as demonstrated by the increase in binding density with more attractive electrostatic interactions.

It is also interesting that these binding densities are higher than previously reported values, especially in the case of the zwitterionic (DOPC) bilayer where the bilayer lipid composition is directly comparable to past experiments.[13,54] The discrepancy could be due to the QCM-D technique because it is an acoustic wave-based sensor that detects the adsorbed mass of $bvPLA_2$ as well as hydrodynamically coupled solvent.[36] Therefore, the adsorbed mass of $bvPLA_2$ is likely to be overestimated from the measurement, which would result in an overestimated packing density as well. However, even if the wet mass of $bvPLA_2$ is 2−5 times greater than its dry mass (~15 200 Da), then the corrected packing density for DOPC would range from ~37 to ~94 lipid headgroups per $bvPLA_2$ molecule, in agreement with the past values.[13,54] Another factor that may explain the discrepancy is bilayer topology. The supported bilayer's planar structure significantly differs from synthetic vesicles,[55] which have a high degree of local curvature and have served as the substrate in past binding studies.[13,54] Membrane curvature has been shown to affect $sPLA_2$ enzymatic activity, so membrane binding of $bvPLA_2$ is possibly influenced as well.[56]

Membrane Binding Causes Nonhydrolytic Bilayer Disruption. Binding of $bvPLA_2$ to highly negatively charged membranes (DOPC/DOPS 80:20 and DOPC/DOPS 70:30) demonstrated similar two-step adsorption and desorption, as described in the last section. However, desorption was significantly greater (230.1−247.8 $ng \cdot cm^{-2}$) for these two more negatively charged membranes (Table 1, column 3). $bvPLA_2$ initially adsorbed with maximum frequency shifts of ~9 Hz (Figure 4f−g), and then desorption began, resulting in final frequency shifts that corresponded to masses less than that of the original platforms (~442.5 $ng \cdot cm^{-2}$). There was up to a 25% decrease in the platform mass

(53) Sauerbrey, G. *Z. Phys.* **1959**, *155*, (2), 206−222.
(54) Jung, L. S.; Shumaker-Parry, J. S.; Campbell, C. T.; Yee, S. S.; Gelb, M. H. *J. Am. Chem. Soc.* **2000**, *122*, (17), 4177−4184.
(55) Sackmann, E. *Science* **1996**, *271*, (5245), 43−48.
(56) Gheriani-Gruszka, N.; Almog, S.; Biltonen, R. L.; Lichtenberg, D. *J. Biol. Chem.* **1988**, *263*, (24), 11808−11813.

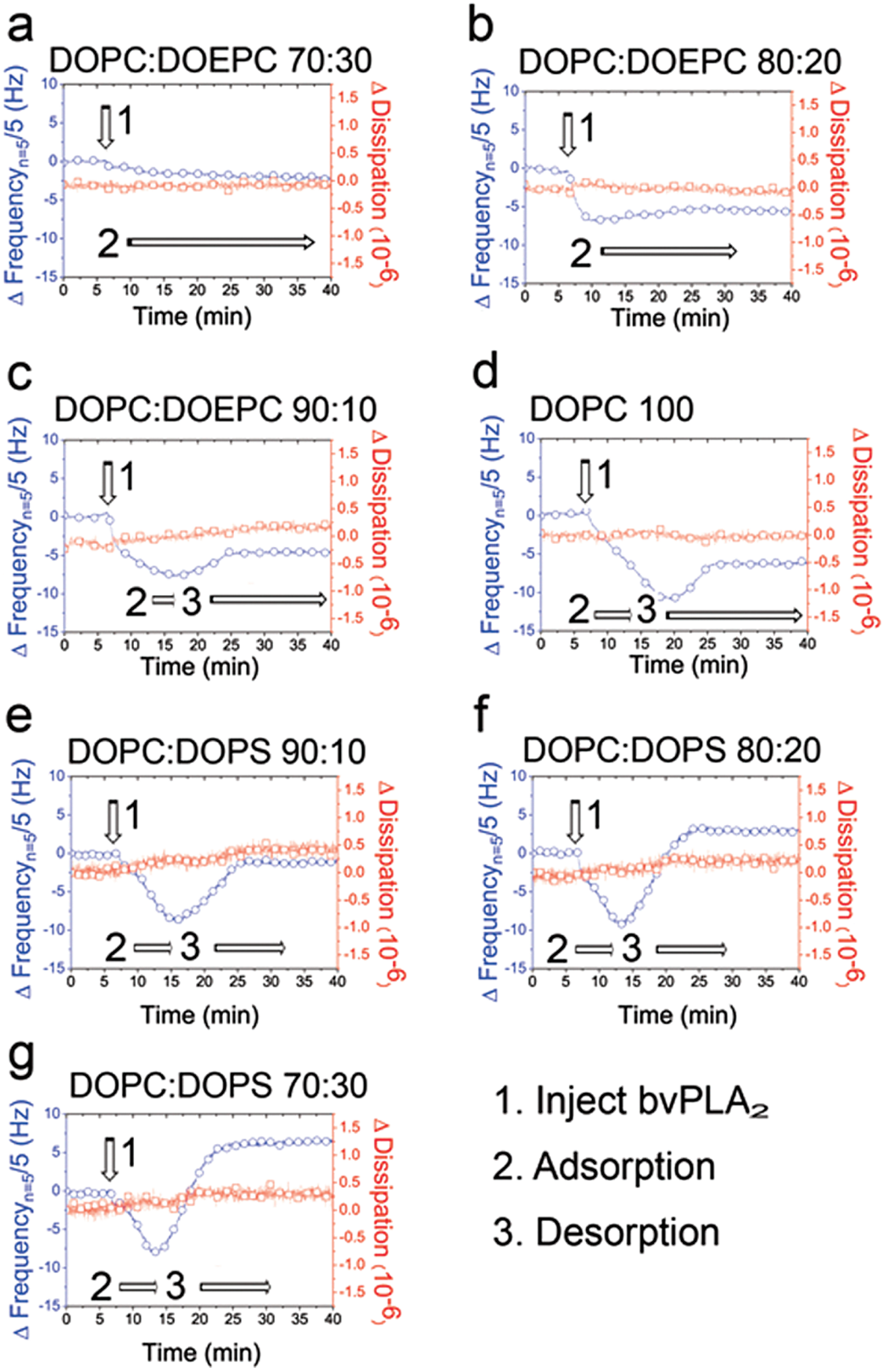

Figure 4. QCM-D monitoring of $bvPLA_2$ interfacial binding under noncatalytic conditions. QCM-D adsorption kinetic data versus time for 0.5 μM $bvPLA_2$ onto supported bilayer platforms of different lipid compositions. After stabilizing the frequency signal (blue) for 5 min, the $bvPLA_2$ solution was injected (arrow 1). Depending on the bilayer platform's lipid composition, the interfacial binding dynamics exhibited adsorption (arrow 2) and, in some cases, desorption (arrow 3) behavior. Note a decrease in frequency indicates an increase in mass on the sensor platform and vice versa. Corresponding energy dissipation versus time plots (red) demonstrate the nonviscoelastic nature of $bvPLA_2$ interfacial binding. (a) DOPC/DOEPC 70:30, (b) DOPC/DOEPC 80:20, (c) DOPC/DOEPC 90:10, (d) DOPC 100, (e) DOPC/DOPS 90:10, (f) DOPC/DOPS 80:20, and (g) DOPC/DOPS 70:30.

Table 1. Summary of QCM-D Binding Experiments[a]

lipid composition (mol %/mol %)		Ads_{Max} ($ng \cdot cm^{-2}$)	Des_{Max} ($ng \cdot cm^{-2}$)	$Ads_{Max} - Des_{Max}$ ($ng \cdot cm^{-2}$)	lipid headgroups (per $bvPLA_2$)
DOPC/DOEPC	70:30	35.4	0.0	35.4	98.9
DOPC/DOEPC	80:20	123.9	17.7	106.2	28.5
DOPC/DOEPC	90:10	132.8	44.3	88.5	27.2
DOPC	100	194.7	70.8	123.9	18.7
DOPC/DOPS	90:10	159.3	123.9	35.4	22.9
DOPC/DOPS	80:20	177.0	230.1	−53.1	20.7
DOPC/DOPS	70:30	247.8	247.8	−106.2	26.0

[a] The interfacial binding of $bvPLA_2$ was quantified in terms of maximum adsorption (column 2) and maximum desorption (column 3) for each bilayer platform. The differences between these values (column 4) are also presented to demonstrate $bvPLA_2$'s bilayer-disrupting activity. While this activity prevented kinetic analysis, it was possible to calculate the number of phospholipid headgroups per $bvPLA_2$ molecule at maximum adsorption (column 5).

as a result of $bvPLA_2$ binding. For DOPC/DOPS 80:20, the binding density (~21 lipid headgroups per $bvPLA_2$ molecule) was in good agreement with the other anionic membranes, but the binding density was significantly lower (~26 lipid headgroups per $bvPLA_2$ molecule) in the case of DOPC/DOPS 70:30 (Table 1, column 5). It is probable that this decrease in binding density is caused by the bilayer-disrupting activity of $bvPLA_2$. Simultaneous $bvPLA_2$ adsorption and bilayer disruption (i.e., lipid desorption) could cause a decreased maximum frequency shift as compared to the maximum binding mass of $bvPLA_2$, resulting in the calculation of a reduced binding density. While other $sPLA_2$s have demonstrated bilayer-disrupting activity,[57,58] this is the first time that the binding interaction of an $sPLA_2$ with a model membrane platform caused a decrease in the platform mass. In contrast to other $sPLA_2$s whose bilayer-disrupting activities are linked to membrane penetration,[57,58] $bvPLA_2$ has been shown to dock at membrane surfaces rather than penetrate.[59,60] One possible explanation is that $bvPLA_2$ tightly binds anionic interfaces, causing bilayer disruption via a phospholipid interaction. Our hypothesis is consistent with past observations that the binding affinity of $bvPLA_2$ increases for more negatively charged bilayers.[26,27]

To further investigate how membrane binding of $bvPLA_2$ under noncatalytic conditions affects its subsequent enzymatic activity, the effects of Ca^{2+} addition were monitored (Supporting Information Figure 3). Depending on the lipid composition, the degree of enzymatic activity significantly varied. $bvPLA_2$ showed a low degree of enzymatic activity toward DOPC/DOEPC 70:30, which is likely due to reduced enzyme binding (Supporting Information Figure 3a) as a result of electrostatic repulsion. Strikingly, the enzyme showed a similar degree of enzymatic activity for lipid bilayers with relatively minor positive and negative surface charges (Supporting Information Figure 3b−e), suggesting that enzymatic activity must be driven by other factors besides solely electrostatic interactions. However, a lower degree of activity was unexpectedly observed for DOPC/DOPS 80:20 and DOPC/DOPS 70:30 (Supporting Information Figure 3f−g). These findings indicate that the binding interaction must affect the enzymatic activity of $bvPLA_2$ by either preventing its activation or inducing a low activity conformation.

Discussion

Interfacial Adsorption Is Not Driven by Electrostatics. The results demonstrate that membrane adsorption of $bvPLA_2$ is not driven primarily by electrostatics. Significant enzyme adsorption ($\Delta f = -11$ to -3 Hz) to supported lipid bilayers with both positive and negative surface charges was detected (Figure 4). This novel finding, that $bvPLA_2$ can bind to positively charged membranes, is surprising because the i-face contains eight basic residues.[59] Binding to a cationic membrane was not expected because the binding interaction would result in repulsive electrostatic interactions that cannot balance the energetically unfavorable desolvation of the i-face and membrane surface associated with membrane binding of $sPLA_2$s.[61] However, since only one basic residue comes into contact with the membrane surface,[59] the other basic residues are likely to remain solvated, reducing electrostatic repulsions. In addition, desolvation is not as significant a factor as with other $sPLA_2$s because $bvPLA_2$ does not penetrate the membrane.[59,60] Therefore, $bvPLA_2$ can bind cationic membranes to some extent.

Although $bvPLA_2$ can bind cationic membranes, the binding density at the point of maximum adsorption (Table 1, column 5) was reduced as compared to anionic membranes, suggesting that electrostatic repulsion does not prevent adsorption but limits the degree of adsorption. Further, membrane binding of $bvPLA_2$ was detected for all lipid compositions, but the total bound mass and type of interaction varied depending on the membrane surface potential, supporting the conclusion that varying the lipid composition affects the nature of the bound enzyme.[62] This finding is in agreement with work by Gadd et al.[52] which determined that snake venom $sPLA_2$ has at least two distinct modes of binding. For DOPC/DOEPC 70:30, $bvPLA_2$ adsorbed monotonically to the supported bilayer, whereas the binding process had two steps for all other bilayers. Despite the differences in the binding interaction that are dependent on the membrane lipid composition, the observation that $bvPLA_2$ can bind to both cationic and anionic membranes demonstrates that the binding process is modulated by nonelectrostatic interactions. Presumably, hydrophobic interactions play a key role in membrane binding since the i-face consists of a large patch of hydrophobic residues.[59]

Desorption Following Membrane Binding Is Driven by Electrostatics. While membrane adsorption of $bvPLA_2$ occurred for all lipid compositions, there was subsequent desorption in only certain cases. For highly negatively charged membranes (DOPC/DOPS 80:20 and DOPC/DOPS 70:30), the binding interaction followed a two-step process. The binding masses of desorption were greater than the binding masses of adsorption,

(57) Wijewickrama, G. T.; Albanese, A.; Kim, Y. J.; Oh, Y. S.; Murray, P. S.; Takayanagi, R.; Tobe, T.; Masuda, S.; Murakami, M.; Kudo, I.; Ucker, D. S.; Murray, D.; Cho, W. *J. Biol. Chem.* **2006**, *281*, (43), 32741−32754.
(58) Chioato, L.; De Oliveira, A. H.; Ruller, R.; Sa, J. M.; Ward, R. J. *Biochem. J.* **2002**, *366*, (Pt 3), 971−976.
(59) Lin, Y.; Nielsen, R.; Murray, D.; Hubbell, W. L.; Mailer, C.; Robinson, B. H.; Gelb, M. H. *Science* **1998**, *279*, (5358), 1925−1929.
(60) Pande, A. H.; Qin, S.; Nemec, K. N.; He, X.; Tatulian, S. A. *Biochemistry* **2006**, *45*, (41), 12436−12447.
(61) Tsai, Y. C.; Yu, B. Z.; Wang, Y. Z.; Chen, J.; Jain, M. K. *Biochim. Biophys. Acta* **2006**, *1758*, (5), 653−665.
(62) Burack, W. R.; Gadd, M. E.; Biltonen, R. L. *Biochemistry* **1995**, *34*, (45), 14819−14828.

indicating that the binding interaction disrupted the bilayer structure by causing lipid desorption (Table 1, column 4). Similar nonhydrolytic bilayer-disrupting activity was also observed for membrane binding of $bvPLA_2$ with bilayers of intermediate surface charge (Figure 4). Interestingly, there is increased desorption for increasingly negatively charged bilayers, which suggests that electrostatic interactions play a key role in driving this behavior. Since $bvPLA_2$ exhibited nonhydrolytic bilayer-disrupting activity toward bilayers not containing DOPS, it is likely that this activity is related to membrane surface charge rather than specific binding of DOPS lipids.

Tatulian et al. demonstrated that negative membrane surface charge can increase the strength of the binding interaction.[21] However, while membrane surface charge modulates desorption (Table 1, column 3), it is likely that this nonhydrolytic activity is driven by more than electrostatics.[26,27] One possible explanation is that the kinetics steps related to interfacial binding and the subsequent binding of an individual phospholipid molecule in the active site are allosterically coupled.[63] Enzyme binding to the membrane interface creates a microenvironment that drives the hydrolysis reaction.[27] Specifically, hydrophobic interactions are believed to be the driving force behind the single lipid molecule binding to the active site.[27] Therefore, even in the absence of the Ca^{2+} cofactor that directs the phospholipid molecule to the active site, hydrophobic interactions could guide an individual phospholipid molecule to bind to the hydrophobic pocket under noncatalytic conditions, but the molecule would be bound in a suboptimal configuration that is not antecedent to the chemical step.

Interfacial Binding under Noncatalytic Conditions Affects Enzymatic Activity. Membrane binding of $bvPLA_2$ under catalytic versus noncatalytic conditions resulted in different enzymatic activities for certain lipid compositions. Under initially noncatalytic conditions, there was significantly reduced enzymatic activity toward DOPS-containing vesicles with increasingly negative surface charge (Figure 3). This finding differs from light scattering experiments where the addition of $bvPLA_2$ under catalytic conditions resulted in increased enzymatic activity toward DOPS-containing vesicles with increasingly negative surface charge (Figure 2). Therefore, membrane binding under noncatalytic conditions must either cause $bvPLA_2$ to adopt a less favorable conformation for enzymatic activity or prevent a Ca^{2+} ion (after Ca^{2+} addition) from entering the active site.

Ahmed et al.[64] suggested a model where interfacial binding of $bvPLA_2$ to the membrane surface may force the enzyme into a low activity conformation. On the basis of the binding affinity of $bvPLA_2$ for negatively charged membranes even under nonhydrolytic conditions, more enzyme molecules would be in a low activity conformation when bound to vesicles with increasing anionic character.[26] Following the addition of Ca^{2+}, there would be lower enzymatic activity against more negatively charged vesicles. This is consistent with the observations of Bell et al.[65] that the initial interaction of the membrane-bound form of snake venom $sPLA_2$ under noncatalytic conditions did not change with the addition of Ca^{2+}. However, it is necessary to further explore how interfacial binding could force the enzyme to adopt a low activity conformation.

A low activity conformation is also consistent with our proposal that $bvPLA_2$ binds an individual phospholipid molecule even in the absence of Ca^{2+}. The bound phospholipid molecule would sterically hinder a Ca^{2+} ion from entering the active site. However, the bound phospholipid molecule would be in equilibrium with bulk phospholipid molecules at the membrane interface. During this exchange between bound and bulk phospholipid molecules, a Ca^{2+} ion associated with the bilayer could enter the hydrophobic pocket and reach the active site,[66] converting the enzyme molecule to its catalytic form. Depending on the strength of the binding interaction, which is related to the membrane surface charge, the exchange rate would vary. In particular, the exchange rate would be lower for more anionic membranes, resulting in slower penetration time of Ca^{2+} on average into the active site and therefore a longer lag period.

Binding Dynamics Guide Interfacial Activation. Our proposed mechanism of membrane binding leading to interfacial activation is a dynamic process that depends on the electrical properties of the membrane. For the first time, we have demonstrated that a $sPLA_2$ can bind to cationic membranes. While the ability of $bvPLA_2$ to bind cationic membranes does not explain its *in vivo* cellular activity, the impact of membrane surface potential on binding dynamics sheds light on its biophysical properties. Another $sPLA_2$ isoform was recently shown to have novel nonhydrolytic membrane-disrupting properties linked to its membrane-penetration ability.[57] However, $bvPLA_2$ binding does not affect the size of vesicles in solution (Supporting Information Figure 1), unlike the other isoform that causes vesicle contraction.[57] The ability of $bvPLA_2$ to disrupt membrane integrity without penetration suggests that while these two isoforms both have membrane-disrupting activity, their modes of action differ.

In this study, we identified two different types of binding interactions depending on membrane electrostatics. Surface charge is a limiting factor in the case of highly cationic membranes, toward which $bvPLA_2$ displays neither hydrolytic nor nonhydrolytic membrane-disrupting activity. Nonetheless, $bvPLA_2$ can bind to these membranes albeit in a distinct state that does not precede interfacial activation. Enzymatic activity is dependent on the type of binding interaction, and the QCM-D results suggest that nonhydrolytic membrane-disrupting activity is a consequence of the distinct bound state leading to interfacial activation.

Depending on the membrane surface charge, $bvPLA_2$ displays weak or strong nonhydrolytic membrane-disrupting activity. One important question is how does the nonhydrolytic membrane-disrupting ability of $bvPLA_2$ relate to its enzymatic activity? We have focused on the interfacial binding step as a part of the more complex interfacial activation process. The substrate model argues that lag time is linked with membrane properties. For example, structural membrane defects or the presence of anionic lipids can reduce or eliminate the lag period before interfacial activation.[35,42,43,52] While previous experiments have demonstrated that membrane electrostatics is linked to the lag phase, there has been little insight into how interfacial binding affects the lag phase. The lag phase is believed to be linked to small-scale lipolysis, which results in a redistribution of products in the membrane that causes structural defects from lateral phase separation as well as an increased anionic surface charge.[35,42,43] Thus, the lag phase is overcome by two interrelated effects. First, the membrane becomes more negatively charged with the production of lysophospholipids, which creates a stronger electrostatic attraction between the membrane and $sPLA_2$s. Second, a consequence of lysophospholipid production is that the membrane becomes more heterogeneous on the local scale, causing

(63) Tatulian, S. A. *Biophys. J.* **2003**, *84*(3), 1773–1783.
(64) Ahmed, T.; Kelly, S. M.; Lawrence, A. J.; Mezna, M.; Price, N. C. *J. Biochem.* **1996**, *120*, (6), 1224−1231.
(65) Bell, J. D.; Biltonen, R. L. *J. Biol. Chem.* **1989**, *264*, (1), 225−230.
(66) McLaughlin, S.; Mulrine, N.; Gresalfi, T.; Vaio, G.; McLaughlin, A. *J. Gen. Physiol.* **1981**, *77*, (4), 445−473.

structural defects. After a critical value of lysophospholipid is produced, the lag period ends and $sPLA_2$ assumes full enzymatic activity.[35]

However, structural defects need not be caused by lateral phase separation. We have demonstrated that the bilayer-disrupting ability of $bvPLA_2$ is related to the membrane surface charge. Since this activity increases toward more negatively charged membranes, it helps to explain how anionic lipids in the membrane reduce the lag period through increased bilayer disruption. Thus, interfacial activation is only indirectly linked to membrane surface charge. The nonhydrolytic bilayer-disrupting activity of $bvPLA_2$ is related to the membrane surface charge and provides the link between anionic lipid composition and membrane structural defects, two known determinants of interfacial activation. The particular dynamics of the interfacial binding step, which depend on the lipid composition, shape the overall interfacial activation mechanism. For negatively charged membranes, interfacial activation is not necessarily caused by lysophosphospholipid production that alters the membrane physical properties but rather through the biophysical interaction between $bvPLA_2$ and the membrane.

Conclusion

Membrane binding of $bvPLA_2$ leading to interfacial activation is a highly dynamic process that consists of at least two steps. Although $bvPLA_2$ can bind to positively charged membranes, the type of interaction is insufficient for bilayer disruption and subsequent interfacial activation. By contrast, $bvPLA_2$ demonstrates bilayer-disrupting activity toward negatively charged membranes, causing structural defects in the membrane structure that have been previously shown to be a determinant of interfacial activation. Therefore, we propose that membrane binding of $bvPLA_2$ is insufficient for interfacial activation. A novel, nonhydrolytic activity of $bvPLA_2$ is required for interfacial activation; this activity acts by causing structural defects in the membrane structure that decreases the lag phase. Further, the relationship between negative membrane surface charge and bilayer-disrupting activity helps explain its enzymatic activity in biological systems. From these findings, new pharmaceutical approaches against $bvPLA_2$ activity can be designed to prevent either membrane adsorption or nonhydrolytic bilayer-disrupting activity, both of which are necessary for enzymatic activity, opening up a new set of specific functional targets for inhibitor design.

Acknowledgment. This work was supported by the NSF-funded Stanford University CPIMA SURE program, the Arnold and Mabel Beckman Foundation, and the HHMI-funded University of Florida Science for Life program. J.A.J. is a recipient of a Beckman Scholars award and an HHMI Science for Life Extramural Research Award. N.J.C. is a recipient of an American Liver Foundation Postdoctoral Fellowship, a Roche Global Postdoctoral Fellowship, and a Stanford Dean's Fellowship.

Supporting Information Available: Membrane binding of $bvPLA_2$ under noncatalytic conditions, characterization of supported lipid bilayer platform, and effects of Ca^{2+} addition to $bvPLA_2$ bound on supported bilayer under noncatalytic conditions. This material is available free of charge via the Internet at http://pubs.acs.org.